Analysis of Resonant Bessel-Beam Launchers based on Isotropic Metasurfaces

Edoardo Negri[1*], Walter Fuscaldo[2†], Mauro Ettorre[3‡], Paolo Burghignoli[4*], Alessandro Galli[5*]
[*]Dipartimento di Ingegneria dell'Informazione, Elettronica e Telecomunicazioni, Sapienza Università di Roma, Rome, Italy, {edoardo.negri[1], paolo.burghignoli[4], alessandro.galli[5]}@uniroma1.it
[†]Istituto per la Microelettronica e Microsistemi, Consiglio Nazionale delle Ricerche, Rome, Italy, walter.fuscaldo@cnr.it[2]
[‡]Université de Rennes, CNRS, IETR (Institut d'Électronique et des Technologies du numéRique), UMR 6164, F-35000 Rennes, France, mauro.ettorre@univ-rennes1.fr[3]

***Abstract*—Resonant Bessel-beam launchers are azimuthally invariant structures characterized by a circular grounded dielectric slab with an isotropic metasurface on top. Previous works analyzed the launchers performance for some specific cases, assuming TE or TM polarizations, inductive or capacitive metasurfaces, cavities with sub-wavelength or half-wavelength height. We show here with both theoretical and full-wave results that the inductive or capacitive nature of the metasurface has a fundamental role in the radiating behavior of these devices. Results are reported for the relevant TM-polarized case, considering air-filled, half-wavelength thick cavities. The extension of this analysis to the TE-polarized and dielectric-filled case will be discussed at the conference.**

***Index Terms*—Bessel beams, leaky waves, plasmonic surface wave, metasurfaces, millimeter waves**

I. Introduction

Various modern applications call for radiating devices capable of focusing the electromagnetic energy in a narrow spatial region at millimeter waves (mm-W). In this regard, the mm-W generation of localized beams [1], and in particular Bessel beams [2], has attracted much interest owing to the limited-diffractive and self-healing properties of such beams [1]. In the last decade, a number of planar structures have been recently proposed at microwaves and mm-W (see, e.g., [3] and refs. therein). A common classification of such structures distinguishes between *resonant* launchers (see, e.g., [4]–[7]) and *wideband* launchers [8], [9]. The former have the advantage of being compact in size, but typically show a narrow fractional bandwidth, the latter present a wideband behavior at the expense of an electrically large aperture size [10].

Here, we will focus only on resonant Bessel-beam launchers (BBLs) with azimuthal symmetry, giving emphasis to some theoretical aspects that were previously neglected, but still have a general character. Indeed, the class of resonant BBLs with azimuthal symmetry comprises different kinds of structures, all sharing the same architecture: a circular grounded dielectric slab with an *isotropic* metasurface on top [11], and excited with a simple dipole-like source at the center. In the literature, these structures are distinguished by the type of the feeder (e.g., a simple coaxial cable [4] for TM-polarized BBs, or a loop antenna [7] for TE-polarized BBs), the metasurface geometry (e.g., square patches [4], or strip gratings [7]), the cavity height (sub-wavelength [4], or half-wavelength [6]).

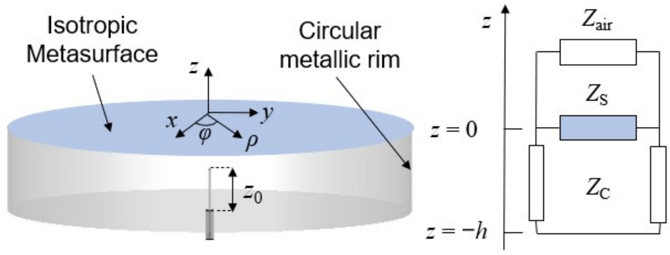

Fig. 1. On the left, a schematic view of a TM polarized Bessel beam launcher centrally fed by a 50-Ω coaxial cable. On the right, its transverse equivalent network. Z_{air} and Z_{C} are the characteristic impedances of the corresponding transmission-line sections.

In this work, we aim at analyzing the differences in the radiating behavior of such BBLs, highlighting the important role played by the inductive/capacitive nature of the isotropic metasurface. We limit the analysis to air-filled $\lambda/2$-thick cavities in the TM case. Interestingly, we will show that when a *capacitive* metasurface is used, care must be taken to the resonances between the *fundamental* leaky mode and the *higher order* leaky mode. The interaction between these two modes can indeed negatively affect the radiating performance. For the same reasons, when an *inductive* metasurface is used, care must be taken to the resonances between a *plasmonic* mode and the *higher order* leaky mode. These findings will be derived in Section II through a theoretical analysis and validated with full-wave simulations in Section III. In Section IV, conclusions are drawn.

II. Theoretical Analysis

The reference structure is represented in Fig. 1 along with the relevant transverse equivalent network (TEN). The central coaxial cable acts as a vertical electric dipole source and thus excites only TM modes supported by the cavity. These partially guided modes can be seen as slight perturbations of those of a radial parallel-plate waveguide (PPW) radiating in free space due to the presence of a partially reflecting sheet (the isotropic metasurface) replacing the top metallic plate of a radial PPW. The electromagnetic properties of the isotropic metasurface are assumed to be fully described by a single scalar purely imaginary impedance sheet $Z_{\mathrm{s}} = jX_{\mathrm{s}}$, where

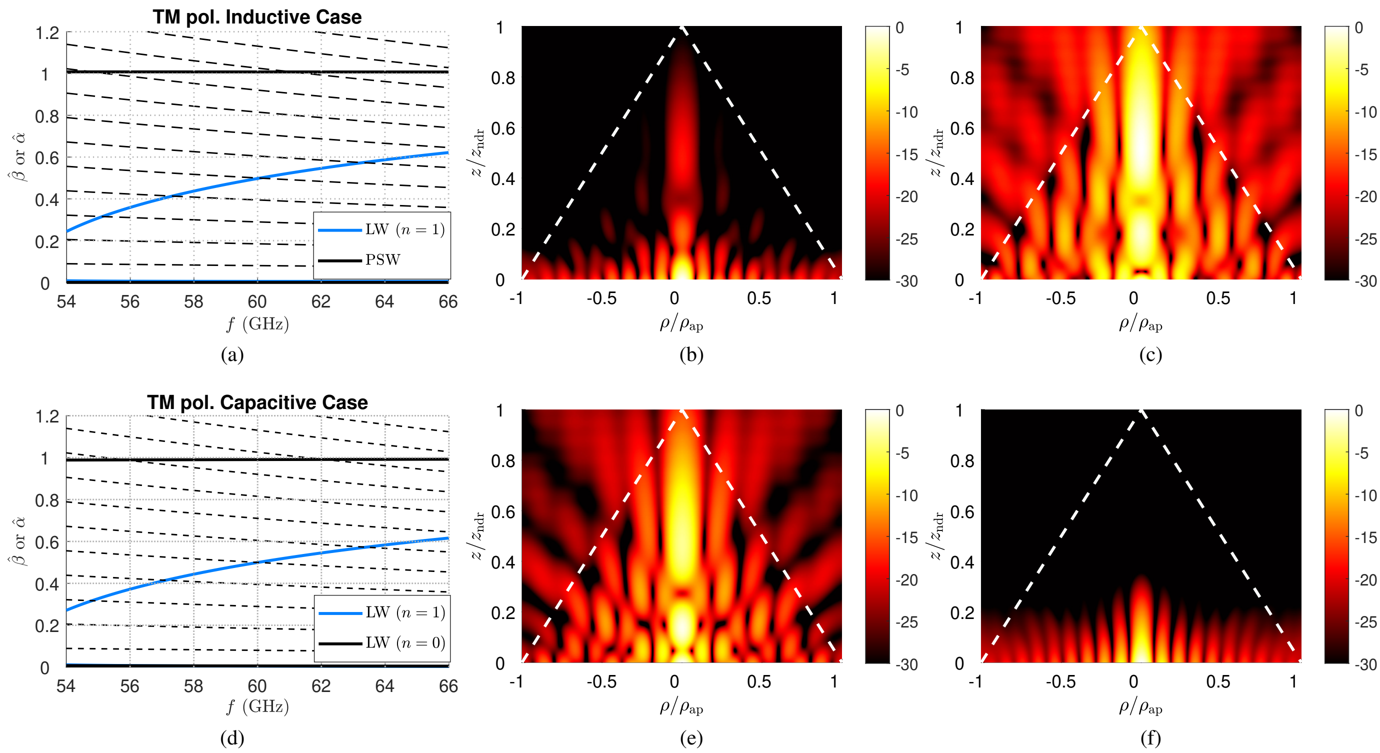

Fig. 2. Results for the BBL with (a)–(c) an inductive metasurface, and (d)–(f) a capacitive metasurface. In (a) and (d) the dispersion diagrams are shown. The radial resonances are reported in black dashed lines, whereas the $n = 1$ leaky mode (labeled as LW) is shown in light blue solid line. Black solid lines are used for the plasmonic mode (labeled as PSW) in (a) and for the $n = 0$ leaky mode in (d). In (b), (c), (e), and (f) the normalized amplitude (in dB) of E_z is shown over a 2-D plane limited along ρ and z by the aperture radius and the nondiffractive range, respectively. Shadow boundaries are reported as white dashed lines. In (b) E_z is evaluated at 60 GHz for the structure having the dispersion reported in (a). In (c) the same result of (b) is shown for a structure with a slightly different choice of the parameters so as to avoid the resonance with the plasmonic mode. In (e) and (f) E_z is evaluated at 60 GHz and 62 GHz for the structure having the dispersion reported in (d). From (e) and (f) it is manifest that at 60 GHz (62 GHz) the higher order (fundamental) leaky mode gives the dominant contribution to the radiation mechanism.

the sign of the reactance X_{s} can be either positive (inductive sheet) or negative (capacitive sheet). In the capacitive case, the height h of the cavity can be set to $h \ll \lambda_0$, λ_0 being the free-space wavelength, if one wants to create a Bessel beam with the fundamental $n = 0$ leaky mode (see, e.g., [4]). When the height is set to $h \simeq \lambda_0/2$, the higher order $n = 1$ leaky mode is excited (see, e.g., [6]), thus one can choose to use either an inductive or a capacitive sheet.

The circular metallic rim is placed at a radial distance ρ_{ap} from the center so as to coincide with one of the zeroes of the stationary Bessel-like distribution that is supported by the cavity [4]. In such a way, a Bessel beam is radiated into the near field, within a conical-shaped region whose apex determines the so-called *nondiffractive* range given by the expression [4]:

$$z_{\text{ndr}} = \rho_{\text{ap}} \text{Re}[k_z]/\text{Re}[k_\rho] \quad (1)$$

where k_z and k_ρ are the generally complex vertical and radial wavenumbers, respectively, related through the separation relation $k_\rho^2 + k_z^2 = k_0^2$, k_0 being the free-space wavenumber. In particular, a zeroth order, azimuthally invariant Bessel beam is created for the vertical electric field component E_z.

The main features of the Bessel beam, namely, the beamwidth and the nondiffractive range, are fully determined by the aperture radius ρ_{ap} and the radial wavenumber $k_\rho = \beta - j\alpha$, where β and α are the phase and attenuation constants, respectively [12]. In [4], closed-form expressions have been derived to set the values of h, X_{s}, and ρ_{ap} to have a desired value of β and α at a given frequency f_0 to generate a zeroth Bessel beam with a prescribed number q of zeroes over the aperture, when generated with the $n = 0$ leaky mode. These formulas have been extended to the generation of Bessel beams with higher order (i.e., $n \neq 0$) leaky modes and experimentally validated for $n = 1$ in [6].

Here we use the formulas in [6, eqs. (12)–(13)] to generate a Bessel beam with $q = 5$ zeroes at $f_0 = 60$ GHz with $\hat{\beta} = 0.5$ and $\hat{\alpha} = 0.005$ (the 'hat' refers to the normalization with respect to k_0), using the $n = 1$ leaky mode in an air-filled cavity (relative permittivity $\varepsilon_{\text{r}} = 1$). This choice leads to $X_{\text{s}} = 32.5\,\Omega$ and $h = 2.79$ mm for the inductive case and $X_{\text{s}} = -34.7\,\Omega$ and $h = 2.98$ mm for the capacitive case, and $\rho_{\text{ap}} = 23.75$ mm in both cases. The accuracy of the formulas can be inferred from the dispersion diagrams reported in Fig. 2(a) and (d) for the inductive and the capacitive case, respectively. The dispersion curves of the leaky modes have been obtained through the application of the transverse resonance technique [13] to the TEN in order to obtain the relevant dispersion equation of the structure, which is then

solved for the complex *improper* roots (i.e, with $\mathrm{Im}[k_z] > 0$) using the Padé algorithm [14]. The dispersion curves for the radial resonances are found from

$$\beta\rho_{\mathrm{ap}} = j_{0q} \tag{2}$$

where j_{0q} is the q-th zero of the zeroth order Bessel function.

Interestingly, Fig. 2(a) and (d) clearly show that the dispersion curves of the $n = 1$ leaky modes (light blue solid lines) intersect the radial resonances (black dashed lines) with $q = 5$ zeroes at 60 GHz. However, in the inductive case (Fig. 2(a)), attention should be paid to the propagation of a plasmonic surface wave (PSW) which is inherently supported by the structure. The dispersion curve of this surface wave mode can be found by solving the dispersion equation for the real *proper* (i.e, with $\mathrm{Im}[k_z] < 0$) roots, using, as an initial guess, the approximate expression of the plasmonic mode propagating on a free-standing inductive sheet [15]:

$$\hat{k}_\rho = \sqrt{1 + (2X_{\mathrm{s}}/\eta_0)^2} \tag{3}$$

where $\eta_0 \simeq 377\,\Omega$ is the free-space impedance. Interestingly, Fig. 2(a) not only shows the presence of PSW mode, but highlights that it resonates with the $q = 10$ radial resonance at $f_0 = 60$ GHz. As a result, it is expected that the simultaneous presence of the leaky mode and the PSW mode resonance at $f_0 = 60$ GHz may have a detrimental effect in the generation of a pure Bessel-beam. This argument will be corroborated in Section III with the help of full-wave simulations, where we will also propose a simple technique to circumvent this issue.

The capacitive case also deserves some attention. As a matter of fact, PSW modes are not supported by capacitive sheets under TM polarization. However, in the capacitive case we have previously commented that a fundamental $n = 0$ leaky mode exists. At higher frequencies, it has been shown [6] that in a dielectric-filled $\lambda/2$-thick cavity loaded with a capacitive sheet, this fundamental TM leaky mode evolves in a TM surface wave that may resonate. Such surface-wave resonances negatively affect the generation of Bessel beams based on the higher order leaky mode. In the air-filled cavity studied here, surface waves do not exist, but at higher frequencies the fundamental leaky mode resonates with $q = 10$ zeroes at around 62 GHz with $\hat{\beta} \to 1$ (see the black solid line in Fig. 2(d)). We will show that the resonance with the fundamental leaky mode may also affect the Bessel-beam generation with the higher order leaky mode.

III. Numerical Results

In this Section III, full-wave results for BBLs under TM polarization in both the inductive and capacitive case are discussed to corroborate the theoretical analysis in Section II. The structure reported in Fig. 1 is designed on CST Microwave Studio [16] modeling the isotropic metasurface by means of a surface impedance boundary condition (SIBC) using the reactance values provided in the Section II. We should stress that the implementation of a SIBC in a full-wave solver may lead to some differences with respect to the design of a realistic isotropic metasurface, yet it produces sufficiently accurate results to corroborate the concept (see, e.g., [4]–[6]). In addition, it is worth noting that CST requires SIBC to have a frequency dispersion that respects Foster's reactance theorem [17]. Therefore, we use $Z_{\mathrm{s}} = j2\pi f L$ and $Z_s = (j2\pi f C)^{-1}$ for the inductive and capacitive case, respectively, fixing the lumped L and C inductance and capacitance so as to match the desired value of Z_{s} at f_0. Common geometries, such as 2-D patch arrays, strip gratings, and fishnet-like metasurfaces [18], [19] exhibit similar dispersive behaviors.

In order to produce a *pure* TM-polarized Bessel beam, we excited the cavity with a central coaxial cable whose inner probe extends within the cavity up to $z_0 = h/2$ (see Fig. 1). The effects of a different choice for z_0 will briefly be outlined at the end of this Section III. It is worthwhile noting that a thorough comparison of the analytical and full-wave input impedance of such kinds of coaxial feeders has already been investigated in [4].

In Fig. 2(b), the contour plots of the amplitude (in dB) of the vertical electric field component E_z at 60 GHz are shown for the inductive case over the domain $\rho < \rho_{\mathrm{ap}}$ and $0 \le z \le z_{\mathrm{ndr}}$. As expected from the dispersion analysis reported in Fig. 2(a), the simultaneous presence of a PSW mode resonating with $q = 10$ zeroes and a higher order leaky mode resonating with $q = 5$ zeroes prevents the generation of a pure Bessel beam with only 5 nulls. As is manifest from Fig. 2(b), the near-field distribution has around 10 nulls in close proximity of the aperture where the surface-wave contribution prevails, and reaches around 5 nulls away from the aperture, where the radiative contribution of the leaky mode prevails over the surface-wave mode. However, the radiating behavior is far from being useful for focusing purposes, the radiating efficiency being poor [20].

In order to avoid this behavior and remove the resonance of the PSW mode at $f_0 = 60$ GHz, the values h and ρ_{ap} of the Bessel beam launcher can properly be tuned. In particular, ρ_{ap} can be changed to shift the radial resonances, whereas h can be adjusted to move the dispersion curve of the leaky mode to obtain approximately the same working point at $f_0 = 60$ GHz. In particular, the choice of $h = 2.742$ mm and $\rho_{\mathrm{ap}} = 25.2$ mm, allows for having the higher order leaky mode resonating at almost the same working point (now $\hat{\beta} = 0.47$ at $f_0 = 60$ GHz where it resonates with $q = 5$ zeroes), while shifting the PSW resonance with $q = 10$ zeroes at around $f = 57.5$ GHz. This *fine tuning* technique has proven to be effective, as can be inferred from Fig. 2(c): the near-field distribution has now five distinct nulls from $z = 0$ to $z = z_{\mathrm{ndr}}$.

We can now examine the capacitive case whose dispersion curve is reported in Fig. 2(d). As opposed to the inductive case, we no longer have a PSW, but the fundamental $(n = 0)$ leaky mode which resonates with $q = 10$ zeroes at $f = 62$ GHz. Since this resonance does not occur at $f_0 = 60$ GHz, the near-field distribution is not much affected, and we can distinguish five nulls as we move sufficiently far from the aperture plane (see Fig. 2(e)). Nevertheless, the beam is not as pure as in Fig. 2(c) where we shifted away the PSW resonance present in the inductive case. The deterioration of the beam can therefore

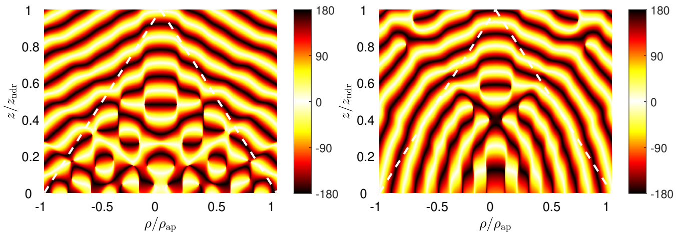

(a) (b)

Fig. 3. The phase (in degrees) of E_z is reported for the capacitive case at (a) 60 GHz, and at (b) 62 GHz. The phase fronts are aligned with a wavenumber that points at (a) 30° and (b) 90°, in agreement with the normalized phase constant $\hat{\beta} \simeq 0.5$ of the $n = 1$ leaky mode at 60 GHz and $\hat{\beta} \simeq 0.991$ of the $n = 0$ leaky mode at 62 GHz. Shadow boundaries are reported as white dashed lines.

be attributed to the presence of this fundamental leaky mode, whose existence is corroborated by Fig. 2(f) which shows the near-field distribution at $f = 62$ GHz, where this mode is supposed to resonate with $q = 10$ zeroes, and the beam has indeed 10 nulls. However, the purity of the beam at the working frequency $f_0 = 60$ GHz can be improved by tuning the positioning of the probe within the cavity. We noted that, in the capacitive case, the purity of the beam is slightly improved for $z_0 = h/4$, whereas it considerably deteriorates for $z_0 = 3h/4$ (not shown for brevity) with respect to the case analyzed here (viz., $z_0 = h/2$). As a matter of fact, this parameter affects the excitation coefficients of the two existing leaky modes. Conversely, in the inductive case, it appears that when the PSW resonates exactly at 60 GHz the near-field distribution is negatively affected, regardless the position of the source. An in-depth investigation on these aspects will deserve further specific attention.

Finally, we report in Fig. 3(a)–(b) the phase (in degrees) of E_z at 60 GHz and 62 GHz, respectively, and for the capacitive case only. The 2-D maps of the phase are useful to corroborate the dispersion analysis as the phase fronts are expected to be orthogonal to the wavevector of the dominant leaky mode. As is well known, the phase constant of the leaky mode is associated to a ray emitted from the aperture at an angle $\theta_0 = \arcsin \hat{\beta}$ (measured from the vertical z-axis). In our case, we have $\hat{\beta} \simeq 0.5$ for $n = 1$ and $\hat{\beta} = 0.991$ for $n = 0$ that generate wave fronts with angles approximately equal to 30° and 90°, as confirmed by the orientation of the phase fronts shown in Fig. 3(a) and Fig. 3(b), respectively.

IV. Conclusion

In this work, we have investigated the role of the inductive/capacitive character of an isotropic metasurface for the realization of TM-polarized Bessel-beam launchers from a theoretical viewpoint. In particular, we demonstrated through a rigorous modal analysis that in the inductive case the presence of a plasmonic mode may interfer with the Bessel-beam generation, whereas in the capacitive case, the simultaneous presence of a fundamental and a higher order leaky mode may have some detrimental effects as well. The consistency of the results has been established through full-wave simulations, and possible techniques to mitigate these issues have briefly been commented. More detailed analyses, such as the extension to the TE-polarized case, as well as the introduction of a dielectric filling and the positioning of the source will be discussed at the conference and analyzed in depth in future works.

References

[1] H. E. Hernández-Figueroa, M. Zamboni-Rached, and E. Recami, *Non-diffracting Waves*. Weinheim, Germany: John Wiley & Sons, 2013.

[2] J. Durnin, "Exact solutions for nondiffracting beams. I. The scalar theory," *J. Opt. Soc. Am. A*, vol. 4, no. 4, pp. 651–654, 1987.

[3] M. Ettorre, S. C. Pavone, M. Casaletti, M. Albani, A. Mazzinghi, and A. Freni, "Near-field focusing by non-diffracting Bessel beams," in *Aperture Antennas for Millimeter and Sub-Millimeter Wave Applications*. Cham, Switzerland: Springer, 2018, pp. 243–288.

[4] M. Ettorre and A. Grbic, "Generation of propagating Bessel beams using leaky-wave modes," *IEEE Trans. Antennas Propag.*, vol. 60, no. 8, pp. 3605–3613, Aug. 2012.

[5] M. Ettorre, S. M. Rudolph, and A. Grbic, "Generation of propagating Bessel beams using leaky-wave modes: experimental validation," *IEEE Trans. Antennas Propag.*, vol. 60, no. 6, pp. 2645–2653, Jun. 2012.

[6] W. Fuscaldo, G. Valerio, A. Galli, R. Sauleau, A. Grbic, and M. Ettorre, "Higher-order leaky-mode Bessel-beam launcher," *IEEE Trans. Antennas Propag.*, vol. 64, no. 3, pp. 904–913, Mar. 2016.

[7] P. Lu, D. Voyer, A. Bréard, J. Huillery, B. Allard, X. Lin-Shi, and X.-S. Yang, "Design of TE-polarized Bessel antenna in microwave range using leaky-wave modes," *IEEE Trans. Antennas Propag.*, vol. 66, no. 1, pp. 32–41, Jan. 2017.

[8] M. Albani, S. C. Pavone, M. Casaletti, and M. Ettorre, "Generation of non-diffractive Bessel beams by inward cylindrical traveling wave aperture distributions," *Opt. Express*, vol. 22, no. 15, pp. 18 354–18 364, 2014.

[9] W. Fuscaldo, D. Comite, A. Boesso, P. Baccarelli, P. Burghignoli, and A. Galli, "Focusing leaky waves: A class of electromagnetic localized waves with complex spectra," *Phys. Rev. Appl.*, vol. 9, no. 5, p. 054005, 2018.

[10] W. Fuscaldo, S. C. Pavone, D. Comite, G. Valerio, M. Albani, M. Ettorre, and A. Galli, "Design criteria of X-wave launchers for millimeter-wave applications," *Int. J. Microw. Wireless Techn.*, vol. 11, no. 9, pp. 939–949, 2019.

[11] S. Tretyakov, *Analytical Modeling in Applied Electromagnetics*. Norwood, MA, USA: Artech House, 2003.

[12] W. Fuscaldo and S. C. Pavone, "Metrics for localized beams and pulses," *IEEE Trans. Antennas Propag.*, vol. 68, no. 2, pp. 1176–1180, Feb. 2020.

[13] R. Sorrentino, "Transverse resonance technique," in *Numerical Techniques for Microwave and Millimeter-Wave Passive Structures*, T. Itoh, Ed. New York, NY, USA: John Wiley & Sons, 1989, ch. 11.

[14] V. Galdi and I. M. Pinto, "A simple algorithm for accurate location of leaky-wave poles for grounded inhomogeneous dielectric slabs," *Microw. and Opt. Technol. Lett.*, vol. 24, no. 2, pp. 135–140, 2000.

[15] S. A. Maier, *Plasmonics: Fundamentals and Applications*. New York, NY, USA: Springer, 2007.

[16] "CST products Darmstadt, Germany, 2019." [Online]. Available: http://www.cst.com

[17] R. E. Collin, *Field Theory of Guided Waves*. New York, NY, USA: McGraw-Hill, 1960.

[18] O. Luukkonen, C. Simovski, G. Granet, G. Goussetis, D. Lioubtchenko, A. V. Raisanen, and S. A. Tretyakov, "Simple and accurate analytical model of planar grids and high-impedance surfaces comprising metal strips or patches," *IEEE Trans. Antennas Propag.*, vol. 56, no. 6, pp. 1624–1632, Jun. 2008.

[19] W. Fuscaldo, S. Tofani, D. C. Zografopoulos, P. Baccarelli, P. Burghignoli, R. Beccherelli, and A. Galli, "Systematic design of THz leaky-wave antennas based on homogenized metasurfaces," *IEEE Trans. Antennas Propag.*, vol. 66, no. 3, pp. 1169–1178, Mar. 2018.

[20] G. Minatti, E. Martini, and S. Maci, "Efficiency of metasurface antennas," *IEEE Trans. Antennas Propag.*, vol. 65, no. 4, pp. 1532–1541, Apr. 2017.